AEDC-TR-70-286

$a_y{}^2$

SUPER- AND SUB-SPECULAR MAXIMA IN THE ANGULAR DISTRIBUTION OF POLARIZED RADIATION REFLECTED FROM ROUGHENED DIELECTRIC SURFACES

A. M. Smith and P. R. Müller

ARO, Inc.

March 1971

VON KÁRMÁN GAS DYNAMICS FACILITY
ARNOLD ENGINEERING DEVELOPMENT CENTER
AIR FORCE SYSTEMS COMMAND
ARNOLD AIR FORCE STATION, TENNESSEE

NOTICES

SUPER- AND SUB-SPECULAR MAXIMA
IN THE ANGULAR DISTRIBUTION OF
POLARIZED RADIATION REFLECTED FROM
ROUGHENED DIELECTRIC SURFACES

A. M. Smith and P. R. Muller
ARO, Inc.

FOREWORD

The research reported herein was sponsored by Headquarters, Arnold Engineering Development Center (AEDC), Air Force Systems Command (AFSC) Arnold Air Force Station, Tennessee, under Program Element 64719F.

The results of the research were obtained by ARO, Inc. (a subsidiary of Sverdrup & Parcel and Associates, Inc.), contract operator of AEDC, AFSC, under Contract F40600-71-C-0002. The work was performed under ARO Project Nos. SW5906 and SW5007 during the period from May 1969, through April 1970. The manuscript was submitted for publication on October 13, 1970.

This technical report has been reviewed and is approved.

Michael G. Buja　　　　　　　　　Harry L. Maynard
First Lieutenant, USAF　　　　　　Colonel, USAF
Research Division　　　　　　　　　Research Division
Directorate of Plans　　　　　　　Director of Plans
　　and Technology　　　　　　　　　　and Technology

ABSTRACT

To study the effects of surface roughness on the reflection of radiation from the vacuum-deposit interface of CO_2 cryodeposits, detailed angular distribution measurements were made of the polarized radiant flux reflected from roughened glass samples which had similar optical properties to CO_2 cryodeposits. As a result of these measurements, a new type of off-specular peak was discovered. This maximum is termed "sub-specular" and occurs for parallel-polarized radiation provided the wavelength and zenith incidence angle are appreciably less than the dielectric's surface roughness and Brewster angle, respectively. If the incidence angle is greater than the Brewster angle, the maximum in the angular distribution is super-specular and occurs even for a surface roughness smaller than the radiation wavelength. No sub-specular maxima are observed for perpendicular-polarized radiation, but super-specular maxima occur for all non-normal incidence angles provided the dielectric's surface roughness is significantly greater than the radiation wavelength, 0.5μ. For reflected radiant flux containing all components of polarization, only super-specular peaks are observed. These peaks occur if the dielectric surface roughness is larger than the radiation wavelength and the incidence angle is equal to or greater than approximately 30 deg. A formula is derived for the radiation reflected in the plane of incidence and is used to quantitatively confirm the existence of the super- and sub-specular maxima for moderate incidence angles. The super- and sub-specular maxima phenomena have potential application to making in situ measurements of surface roughness characteristics.

CONTENTS

APPENDIX
ILLUSTRATIONS

Figure

SECTION I
INTRODUCTION

Off-specular maxima in the directional distributions of radiant flux or intensity reflected from rough dielectric surfaces have been reported by numerous investigators since the early part of this century. Moreover, in recent years, this off-specular peak phenomenon has been experimentally (Refs. 1 and 2) and theoretically (Refs. 3, 4, 5, and 6) studied in considerable detail for both mixed (containing all polarization components) and plane-polarized reflected radiation. For given zenith incidence angles, the off-specular peaks discussed in these studies occurred in the incidence plane at zenith reflection angles greater than the corresponding specular reflection angles and hence may be referred to as "super-specular" maxima.[1] Similar super-specular maxima have been observed in the AEDC laboratory for a CO_2 cryodeposit dielectric which had a rough surface and significant internal scattering (Ref. 7).

To study this super-specular peak phenomenon for a dielectric with negligible internal scattering and a rough surface of known roughness, detailed angular distribution measurements were made of the radiant flux reflected from roughened glass samples which had optical properties similar to CO_2 cryodeposits and allowed mechanical measurements of the rms surface roughness. These distribution measurements were made in the forward reflection quadrant of the plane of incidence. The objective of this work is to report on a new type of off-specular maximum which was discovered as a result of the above measurements. This new off-specular maximum is termed "sub-specular" since, for a given zenith incidence angle, it occurs in the reflected flux distribution at a zenith reflection angle which is smaller than the specular reflection angle.

The effects of polarization. zenith incidence angle, and sample surface properties on the existence and zenith angular location of both the sub-specular and super-specular reflection maxima have been investigated, and the results are presented. Also, an analytical expression has been formulated for the reflection of radiant flux from a randomly rough dielectric surface having a normal distribution of surface heights. This relation applies to reflection in the plane of incidence and is used to quantitatively predict the existence of the sub-specular and super-specular maxima. Both the discovery of the sub-specular maxima and the accompanying detailed investigation of it are significant contributions toward understanding and exploiting the various phenomena observed in angular distribution measurements of radiation reflected from rough dielectric surfaces.

SECTION II
APPARATUS AND TEST SAMPLES

All measurements of the angular distribution of radiation reflected from the roughened glass surfaces were made using the apparatus shown schematically in Fig. 1 (Appendix). With this system. unpolarized light from a tungsten-halogen lamp was collimated by a series of apertures, chopped mechanically at a frequency of 13 Hz, and then reflected from a plane first surface mirror onto a spherical mirror in the near-normal direction.

---

[1]Zenith incidence and reflection angles are measured relative to the normal of the mean surface.

This mirror focused the radiation on the sample surface at a zenith incidence angle with an incident solid angle $\Delta\omega_i$ of 0.017 sr (see inset, Fig. 1). The sample was vacuum-mounted on a sample holder which was located along with the other aforementioned components on a turntable having an angle indexing device. This sample holder (shown also in Fig. 1) could be adjusted to maintain the roughened surface of the sample on the axis of rotation of the turntable. It also allowed the zenith incidence angle of the irradiance to be set at any desired value within an accuracy of ±0.5 deg. As noted previously, all zenith angles are measured relative to the outward normal of the mean surface.

The radiant flux reflected from the illuminated area of the sample surface in the direction defined by the zenith reflection angle θ and the plane of incidence was collected by a spherical mirror subtending a solid angle of $\Delta\omega_r = \Delta\omega_i = 0.017$ sr. This radiation was focused on the entrance slit of a monochromator after reflection from a plane first surface mirror and transmission through a polarizer. Since the over-detection measurement technique was used, the monochromator entrance slit was set to a slightly greater width than the focused image of the illuminated area of the sample. The monochromator was a standard Perkin-Elmer Model 98 equipped with a CaF_2 prism and a 1P28 photomultiplier detector.

All test samples were glass disks 2.5 cm in diameter and 6 mm thick. The glass was of optical quality and had a refractive index of n = 1.51 ±0.01 at the wavelength λ used in this investigation, 0.5μ. Initially, both sides of each disk were polished flat by use of a standard optical polishing technique. Then, using a similar technique, one side of the disk was roughened by grinding it with an abrasive. This was done for five samples using different size abrasives for each sample. The resulting rms mechanical surface roughness σ_m of each of the five samples was measured with a profilometer, and the following values were recorded: 0.34, 0.63, 1.77, 3.35, and 5.22μ. After these measurements had been performed, the highly polished side of each of the glass disks was coated with a flat black paint of epoxy resin base which had a refractive index of 1.48 ± 0.03. Since this refractive index is effectively equal to that of the glass, a negligible amount of radiation was internally reflected at the glass-paint interface with the radiation transmitted into the paint being absorbed by the pigment particles suspended in the epoxy base. Thus, the problem of internal reflection from the rear side of the transparent sample was essentially eliminated.

SECTION III
PROCEDURE

After alignment and calibration of the irradiation and detection optics, a roughened glass sample was attached to the sample holder and the zenith angle of the incident radiation set to some desired value ψ. Then, using the polarizer, the radiant flux reflected from the sample surface in a specific θ direction was alternately resolved into components polarized perpendicular and parallel to the plane of incidence. Each of these polarized radiation components was transmitted through the monochromator to the photomultiplier detector. A conventional strip-chart recorder was used to display the detector outputs after amplification and/or rectification and filtering. Since the monochromator had a 22-percent greater measured transmission for parallel-polarized radiation, the detector

output recorded for the perpendicular-polarized component was multiplied by 1.22 before comparing it with the detector output obtained for the parallel-polarized component. This unequal transmission of the monochromator for perpendicular- and parallel-polarized radiation is due to differential reflection of these two polarized radiation components at the prism faces (Ref. 2).

After the above-described measurement was completed, the turntable was rotated and the polarized radiant fluxes reflected from the sample surface in another θ direction were determined. This was subsequently done for values of θ ranging from 0 to 90 deg in increments of 5 deg. Also, in the vicinity of all maxima, measurements were made for increments in θ of 0.5 or 1 deg. Then, the zenith incident angle of irradiance was set to a new desired value, and the procedure was repeated. Zenith incidence angles ranging from 10 to 76 deg were used. All measurements were made at a wavelength of 0.5μ.

SECTION IV
EXPERIMENTAL RESULTS

Some results of the angular distribution measurements described in the previous section are shown in Figs. 2, 3, and 4. The data presented are for glass samples with surface roughness σ_m of 0.34, 1.77, and 3.35μ. In each figure, graphs are given for both the parallel (p) and perpendicular (s) polarization components of the reflected radiation. The distribution data shown are presented in the normalized form $\rho_p(\psi,\theta) \cos \theta / \rho_p(\psi,\psi) \cos \psi$ and $\rho_s(\psi,\theta) \cos \theta / \rho_s(\psi,\psi) \cos \psi$ where $\rho_p(\psi,\theta)$ and $\rho_s(\psi,\theta)$ are, respectively, the p- and s-polarized biangular reflectances defined in Ref. 2. This normalization of the reflectance curves by their values at the specular reflection angles $\theta = \psi$ is employed to emphasize the off-specular peaks. The relative magnitude of the off-specular peaks in the p- and s-polarized components of the reflected radiant flux will be shown later.

It is observed in Figs. 2, 3, and 4 that, for some zenith incidence angles ψ, the maxima of the reflected flux distributions occur at zenith reflection angles θ_m greater than the specular reflection angles (super-specular maxima), while for other zenith incidence angles, the maxima of the reflected flux distributions occur at zenith reflection angles θ_m smaller than the specular reflection angles (sub-specular maxima). As seen from Figs. 3 and 4, the sub-specular maxima occur in the angular distributions of p-polarized reflected flux when the irradiance zenith angles are less than 50 deg and the sample surface roughness σ_m is significantly larger than the radiation wavelength, $\lambda = 0.5$. Figure 2 shows that no sub-specular maxima occur when the sample surface roughness is less than the radiation wavelength. However, for zenith incidence angles greater than about 50 deg, super-specular maxima exist in the distributions of p-polarized reflected flux even though the sample surface roughness is smaller than the radiation wavelength. Similar super-specular maxima are observed in the distributions of p-polarized reflected flux for the rougher sample surfaces as seen in Figs. 3 and 4. Super-specular maxima also occur in the directional distributions of the s-polarized reflected flux when the surface roughness of the sample is significantly larger than the radiation wavelength. These super-specular maxima are observed in the results given in Figs. 3 and 4 and occur for all zenith incidence angles. As can be seen from Fig. 2, super-specular maxima are not observed in the angular distributions of s-polarized reflected flux when the sample roughness is less than the radiation wavelength.

More detailed scrutiny of the p-polarized results shown in Figs. 2, 3, and 4 indicates that the distributions change dramatically as the irradiance incidence angle ψ ranges from below the Brewster angle of the glass (ψ_{Br} = 56.5 deg) to slightly above it. For example, in Fig. 2, the ψ = 40 deg distribution exhibits only a specular peak, but the ψ = 50 deg distribution contains both a specular peak and an emerging super-specular maximum, while the ψ = 60 deg distribution has only a super-specular maximum. Moreover, in Figs. 3 and 4, the ψ = 40 deg distributions have a very definite sub-specular maximum, while the ψ = 50 deg distributions exhibit an arising super-specular maximum which becomes fully emerged in the ψ = 60 deg distributions.

Because of the interesting behavior of the p-polarized distributions for irradiance angles near the Brewster angle, further directional distribution measurements were made for closely spaced angles of incidence between 40 and 60 deg. The unnormalized results of these measurements for p-polarized reflected flux are shown in Figs. 5, 6, and 7 for surface roughnesses σ_m of 0.34, 1.77, and 3.35μ, respectively. It is seen in Fig. 5, which is for a σ_m/λ of 0.68, that the specular peak diminishes with increasing incidence angle and vanishes when the incidence angle reaches the Brewster angle. This behavior is consistent with the incidence angle dependence predicted for the p-polarized specular reflectance of a rough dielectric surface with normally (gaussian) distributed surface heights (Refs. 8 and 9), $F_p(\psi,n) \exp[-(4\pi\ \sigma\ \cos\ \psi/\lambda)^2]$. Here σ is the rms value of the surface heights and $F_p(\psi,n)$ is the p-polarized component of the Fresnel reflectance for a smooth dielectric surface (Ref. 10).

It is further observed in Fig. 5 that, for an incidence angle of 46 deg, an emerging super-specular maximum appears in the p-polarized distribution at $\theta_m \simeq$ 70 deg. This super-specular maximum grows in prominence as the incidence angle is increased but remains at essentially the same angular location, θ_m = 72 deg (see dashed curve C-D). In Fig. 6, which is for a σ_m/λ of 3.54, the sub-specular maximum observed in the distribution for ψ = 40 deg diminishes in the distributions for increasing incidence angles (see dashed curve A-B), while a super-specular maximum emerges and continues to increase in magnitude (see dashed curve C-D). It is seen that, for incidence angles below 48 deg, only sub-specular maxima appear in the distributions, while, for incidence angles above 54 deg, solely super-specular maxima are observed. For incidence angles from 48 to 52 deg, the distributions have both sub- and super-specular maxima. In Fig. 7, which is for a σ_m/λ of 6.77, the distributions do not simultaneously exhibit sub-specular and super-specular maxima for any angle of incidence. Hence, this makes it appear that the sub-specular maximum in the distributions changes continuously to a super-specular maximum with increasing incidence angle. However, it is felt that distributions with simultaneous super- and sub-specular maxima are not observed because the increased contribution of multiple reflections to the distributions for the rougher surface (Ref. 11) obscures the two separate maxima. Such speculation is further confirmed by noting in Fig. 7 that there is a very large change (24 deg) in the angular locations of the maxima of the distributions as the incident angle decreases from 49 to 53 deg. This large change for σ_m = 3.35μ is even more apparent in Fig. 8 which will be presented next.

Figure 8 shows the experimentally determined angular displacements (relative to the specular angle) of the sub- and super-specular maxima in the directional distributions of

4

p- and s-polarized reflected fluxes for roughened glass surfaces. The magnitude of these angular displacements for 0.5μ wavelength radiation is displayed as a function of irradiance zenith angle ψ with sample surface roughness σ_m taken as a parameter. From the results shown, it would appear that when super- and sub-specular maxima occur, their angular displacements (relative to the specular direction) will be greater for rougher surfaces and higher incidence angles until the surfaces become rough enough and/or the incidence (and reflection) angles large enough that multiple reflections (Refs. 4, 5, and 11) and bistatic shadowing (Refs. 3 to 6 and 11 to 13) begin to significantly modify the distributions and affect the locations of their maxima. Then, for larger incidence (and reflection) angles and/or rougher surfaces, the angular displacements of the sub- and super-specular maxima will decrease because of the increased effects of bistatic shadowing (Refs. 4 and 13) and multiple reflections (Refs. 4 and 11).

SECTION V
THEORY AND COMPARISON WITH DATA

To theoretically confirm the existence of the sub-specular peaks, a simple analytical expression will be formulated for the reflection of radiant flux from a rough dielectric surface into the plane of incidence. To do this, it is first necessary to make several assumptions about the characteristics of the surface. One of these is that the rough surface is isotropic. Another is that the surface is randomly rough. The surface heights $\zeta(x)$ of this surface are shown in Fig. 9 and are considered to have a normal distribution

$$W(\zeta) = \frac{1}{\sigma(2\pi)^{1/2}} \exp\left(-\frac{\zeta^2}{2\sigma^2}\right) \qquad (1)$$

with standard deviation σ and correlation function after Beckman (Ref. 9) $B(\tau)$. Since the mean level of the surface $\langle\zeta\rangle = 0$, the standard deviation σ is also the rms value of the surface heights. Now, as indicated by Beckmann (Refs. 9 and 13), $\zeta'(x)$ also has a normal distribution

$$W(\zeta') = \frac{1}{(2\pi|B''(0)|^{1/2})} \exp\left(-\frac{(\zeta')^2}{2|B''(0)|}\right) \qquad (2)$$

with mean value zero and variance $|B''(0)|$ where $(|B''(0)|)^{1/2} = m$ is the rms slope of the surface. Furthermore, he shows (Ref. 9) that this distribution function can be transformed to yield the distribution of surface slopes a, defined (Ref. 9) by $\tan a = \zeta'(x)$. The resulting distribution of the slopes a of a normally distributed surface is given by

$$P(a,m) = \frac{\sec^2 a}{m(2\pi)^{1/2}} \exp\left(-\frac{\tan^2 a}{2m^2}\right) \qquad (3)$$

Note from Fig. 9 that a is also equal to the angle between the normal-to-a local surface slope and the normal-to-the mean plane of the surface.

5

After determining the distribution of slopes of the normally distributed rough surface, a formula can be derived for the reflection of radiation into the plane of incidence. This has been done using essentially the approach employed in Ref. 3 for the v-grooved facet model of a rough surface. Thus, the wavelength λ of the radiation is considered to be small compared with the rms surface heights (σ) and the derivation is based on geometrical optics.[2] In addition, the basic reflection model for the random rough surface assumes specular reflection from the local surface slopes, as shown in Fig. 9, plus a contribution due to the multiple reflections (Ref. 11) which occur when a ray strikes more than one slope before leaving the surface. Also accounted for is "bistatic" shadowing, i.e., the screening of local surface slopes by adjacent surface slopes interrupting the incident and once-reflected radiant flux (Ref. 13). There are, however, several differences between the approach used in Ref. 3 and that employed here. One is that the multiple reflections contribution is not considered to always be perfectly diffuse. This is in agreement with previous experimental results for roughened glass (Ref. 12). Another difference is that it is not necessary to consider that each slope has the same area as was assumed for the facets in Ref. 3. The relaxation of this assumption is made possible through use of the area relationship given in Refs. 14 and 15. A third difference is that the bistatic shadowing function $S(\psi,\theta,m)$ employed here is for a normally distributed rough surface (Ref. 13) and depends on the rms slope of the surface while the $G(\psi,\theta)$ function used in Refs. 3 and 6 for the v-grooved facet surface is independent of the parameter c characterizing the rms slope of the facets.

The result of the above described derivation is

$$\rho(\psi,\theta) = \frac{F(\psi + a, \cdot m)\ P(a,m)\ S(\psi,\ \theta,m)}{4\cos\theta\cos\psi} + b(\psi,\ \theta,m) \tag{4}$$

where $\rho(\psi,\theta)$ is the bidirectional reflectance defined in Refs. 2 and 3 for mixed radiation. Here, $b(\psi,\theta,m)$ is the multiple reflection contribution to the bidirectional reflectance, $P(a,m)$ is the distribution of slopes given in Eq. (3) with $a = (\theta - \psi)/2$ (see Fig. 9), and $F(\psi, + a,n)$ is the Fresnel reflectance for local incidence angle $\psi + a$, where $F(\psi + a,n) = [F_s(\psi + a,n) + F_p(\psi + a,n)]/2$ with F_s and F_p being, respectively, the s- and p-polarized components of the Fresnel reflectance (Ref. 10). The $S(\psi,\theta,m)$ function in Eq. (4) is Beckmann's bistatic shadowing relation for a normally distributed rough surface (Ref. 13) and has the form

$$S(\psi,\ \theta,m) = \begin{cases} S(\psi,m)\ \ S(|\theta,m), & -\pi/2 < \theta < -\psi \\ S(\psi,m) & , -\psi < \theta < 0 \\ S(\psi,m)\ \ S(\theta,m), & 0 < \theta < \pi/2 \end{cases} \tag{5}$$

---

[2]The use of geometrical optics to explain the super-specular peak phenomenon for rough glass surfaces was experimentally investigated in Ref. 14 and found to be valid even for rough surfaces not obeying the condition $\sigma/\lambda \gg 1$.

where

$$S(\psi,m) = \exp\left[-\frac{1}{4} \tan \psi \operatorname{erfc}\left(\frac{\cot \psi}{(2)^{1/2} m}\right)\right] \tag{6}$$

and

$$S(\theta,m) = \exp\left[-\frac{1}{4} \tan \theta \operatorname{erfc}\left(\frac{\cot \theta}{(2)^{1/2} m}\right)\right] \tag{7}$$

It is further noted in Eq. (4) that the multiple reflections contribution $b(\psi,\theta,m)$ has not been assumed perfectly diffuse and is also considered to be a function of the incidence angle ψ and the root-mean-square slope m. This is in agreement with the experimental results of Refs. 11 and 12 and also can be inferred from the theoretical results of Ref. 4. Now, since $\rho(\psi,\theta) = [\rho_s(\psi,\theta) + \rho_p(\psi,\theta)]/2$ for unpolarized incident radiation (Refs. 2 and 6) and $F(\psi + a,n) = [F_s(\psi + a,n) + F_p(\psi + a,n)]/2$, Eq. (4) can be resolved into separate expressions for the plane-polarized bidirectional reflectances $\rho_s(\psi,\theta)$ and $\rho_p(\psi,\theta)$. These are

$$\rho_s(\psi,\theta) = \frac{F_s(\psi + a, n)\, P(a,m)\, S(\psi, \theta, m)}{4 \cos \theta \cos \psi} + b(\psi, \theta, m) \tag{8}$$

and

$$\rho_p(\psi,\theta) = \frac{F_p(\psi + a, n)\, P(a,m)\, S(\psi, \theta, m)}{4 \cos \theta \cos \psi} + b(\psi, \theta, m) \tag{9}$$

Note that the multiple reflections contribution $b(\psi,\theta,m)$ in Eqs. (8) and (9) is assumed to be unpolarized. This is in agreement with the results of Ref. 12.

Equations (4), (8), and (9) with $b(\psi,\theta,m) = 0$ have been used to theoretically predict the experimental distributions of the mixed and plane-polarized reflected fluxes for the glass sample with roughness $\sigma_m = 1.77\mu$ and refractive index n = 1.51. As seen in Figs. 10 and 11, this was done for incidence angles of 20 and 30 deg, respectively, and an rms slope m of 0.247. The experimental (solid) and theoretical (dashed) curves shown are presented in the normalized forms $\rho_p(\psi,\theta) \cos \theta / \rho(\psi,\psi) \cos \psi$, $\rho_s(\psi,\theta) \cos \theta / \rho(\psi,\psi) \cos \psi$, and $\rho(\psi,\theta) \cos \theta / \rho(\psi,\psi) \cos \psi$ for p-polarized, s-polarized, and mixed radiant fluxes, respectively, where $\rho(\psi,\psi)$ is the value of $\rho(\psi,\theta)$ at $\theta = \psi$. This mode of normalization is used to show the relative magnitudes of the sub-specular maximum in the p-polarized distribution and the super-specular maximum in the s-polarized distribution. The sub-specular maximum seen in the distributions for $\psi = 20$ and 30 deg is smaller than the corresponding super-specular maximum, but it does have a significant magnitude relative to that of the super-specular maximum. It is further noted in Figs. 10 and 11 that there is excellent agreement between the theoretical and experimental distributions for reflection angles in the locality of the peaks and for the smaller reflection angles. The agreement is not as good for large reflection angles, and this is attributed to the multiple reflections contribution $b(\psi,\theta,m)$ being neglected. Nevertheless, the excellent

agreement between the analytical and experimental results for zenith reflection angles at and around the peaks of the distributions quantitatively confirms the existence of the sub- and super-specular maxima for moderate incidence angles.

Figure 12 presents the theoretical p-polarized flux distributions for zenith incidence angles near the Brewster angle of the glass, 56.5 deg. The multiple reflections contribution $b(\psi,\theta,m)$ and the rms slope m of the rough surface are again taken as zero and 0.247, respectively. It is seen in Fig. 12 that, as the incidence angle increases, the sub-specular maximum in the p-polarized distributions diminishes, while a super-specular maximum emerges and increases in prominence. For incidence angles below 55 deg, the sub-specular maximum has the greater magnitude, but for incidence angles above 55 deg, the super-specular maximum is larger. The sub- and super-specular maxima are of equal magnitude for ψ = 55 deg. From these results, it can be concluded that the sub-specular maximum in the p-polarized distributions does not change continuously to a super-specular maximum as the incidence angle increases but that the super-specular maximum develops separately as the sub-specular maximum diminishes. The results corroborate the previous discussion regarding the development and demise of the super- and sub-specular maxima in the experimental distributions of Figs. 6 and 7.

Figure 13 presents a comparison between the angular locations θ_m of the off-specular maxima of the experimental and theoretical distributions for the glass sample with roughness σ_m = 1.77μ. These results were obtained from s- and p-polarized reflected flux distributions for incidence angles of 10 to 70 deg. As before, the theoretical flux distributions were for an rms slope m of 0.247 and a refractive index n equal to that of the glass, 1.51. Also, the multiple reflections contribution was again neglected, and hence $b(\psi,\theta,m)$ in Eqs. (8) and (9) was taken equal to zero. It is observed in Fig. 13 that there is good agreement between the theoretical (dashed) and experimental (solid) curves for the angular locations of the super-specular maxima of the s-polarized distributions. This is seen to be true for all incidence angles but especially so for the smaller ones. There also is good agreement between the theoretical and experimental curves for the angular locations of the off-specular maxima of the p-polarized distributions except for the range of zenith incidence and reflection angles where the local incidence angles $\psi + a = (\psi + \theta)/2$ are near the Brewster angle.[3] For these local incidence angles, $F_p(\psi + a,n)$ is quite small, and the multiple reflections contribution can significantly modify the p-polarized distributions and appreciably affect the location of their maxima. Since the multiple reflections contributed were neglected in obtaining the analytical results presented in Fig. 13, good agreement between these results and the p-polarized experimental data are not expected for local incidence angles near the Brewster angle.

SECTION VI
CONCLUSIONS

From the experimental and analytical results presented in the previous sections, it can be concluded that sub-specular maxima occur in the angular distributions of

---

[3]The dotted portions of the theoretical curves for p-polarized radiation denote secondary maxima. For examples of such maxima, see Fig. 12.

parallel-polarized reflected flux for rough dielectric surfaces. These sub-specular maxima are observed if the irradiance zenith angle is appreciably less than the dielectric's Brewster angle and the rms mechanical surface roughness of the dielectric is significantly larger than the radiation wavelength. It is also concluded that super-specular maxima occur in the distributions of parallel-polarized reflected flux when the irradiance zenith angle is greater than the Brewster angle of the dielectric. These super-specular maxima in the p-polarized reflected flux distributions are observed even for an rms mechanical surface roughness less than the radiation wavelength. It is further concluded from the aforementioned results that super-specular maxima occur in the angular distributions of perpendicular-polarized reflected flux for roughened dielectric surfaces. These super-specular maxima in the s-polarized reflected flux distributions are observed for irradiance zenith angles ranging from 10 to 76 deg when the rms mechanical surface roughness of the dielectric is appreciably larger than the radiation wavelength.

REFERENCES

1. Torrance, K. E. and Sparrow, E. M. "Off-Specular Peaks in the Directional Distribution of Reflected Thermal Radiation." Journal of Heat Transfer. Vol. 88, Series C. No. 2, May 1966, pp. 223-230.

2. Torrance, K. E., Sparrow, E. M., and Birkebak, R. C. "Polarization, Directional Distribution, and Off-Specular Peak Phenomena in Light Reflected from Roughened Surfaces." Journal of the Optical Society of America. Vol. 56, No. 7, July 1966. pp. 916-925.

3. Torrance, K. E. and Sparrow, E. M. "Theory for Off-Specular Reflection from Roughened Surfaces." Journal of the Optical Society of America, Vol. 57, No. 9, Sept. 1967, pp. 1105-1114.

4. Nelson, H. F. "Ray Reflection from Rough Dielectric Surfaces." AA & ES 66-5, Nov. 1966, Purdue University, Lafayette, Ind.

5. Nelson, H. F. and Goulard, R. "Reflection from a Periodic Dielectric Surface." Journal of the Optical Society of America. Vol. 57, No. 6, June 1967, pp. 769-771.

6. Torrance, K. E. "Theoretical Polarization of Off-Specular Reflection Peaks." Journal of Heat Transfer. Vol. 91, Series C, No. 2, May 1969, pp. 287-290.

7. Smith, A. M., Tempelmeyer, K. E., Muller, P. R., and Wood, B. E. "Angular Distribution of Visible and Near IR Radiation Reflected from CO_2 Cryodeposits." AIAA Journal, Vol. 7, No. 12, Dec. 1969, pp. 2274-2280.

8. Davies, H. "The Reflection of Electromagnetic Waves from a Rough Surface." Proceedings of the Institution of Electrical Engineers, Part 1V, Vol. 101, No. 7, Aug. 1954, pp. 209-214.

9. Beckmann, P. and Spizzichino, A. The Scattering of Electromagnetic Waves from Rough Surfaces, Macmillan, New York, 1963.

10. Hottel, H. C. and Sarofim, A. F. Radiative Transfer, McGraw-Hill, New York, 1967.

11. Tanaka, S. "Measurement of Reflection Characteristics of Ground Glass Using Polarized Light." Oyo Butsuri, Vol. 26, No. 3, March 1957, pp. 85-91.

12. Tanaka, S. "Reflection Characteristics of Nonmetallic Diffusing Surfaces." Oyo Butsuri, Vol. 28, No. 9, Sept. 1959, pp. 508-514.

13. Beckmann, P. "Shadowing of Random Rough Surfaces." IEEE Transactions on Antennas and Propagation, Vol. AP-13, No. 3, May 1965, pp. 384-388.

14. Voishvillo, N. A. "Reflection of Light by a Rough Glass Surface at Large Angles of Incidence of the Illuminating Beam." Optics and Spectroscopy, Vol. 22, No. 6, June 1967, pp. 517-520.

15. Rense, W. A. "Polarization Studies of Light Diffusely Reflected from Ground and Etched Glass Surfaces." Journal of the Optical Society of America, Vol. 40, No. 1, Jan. 1950, pp. 55-59.
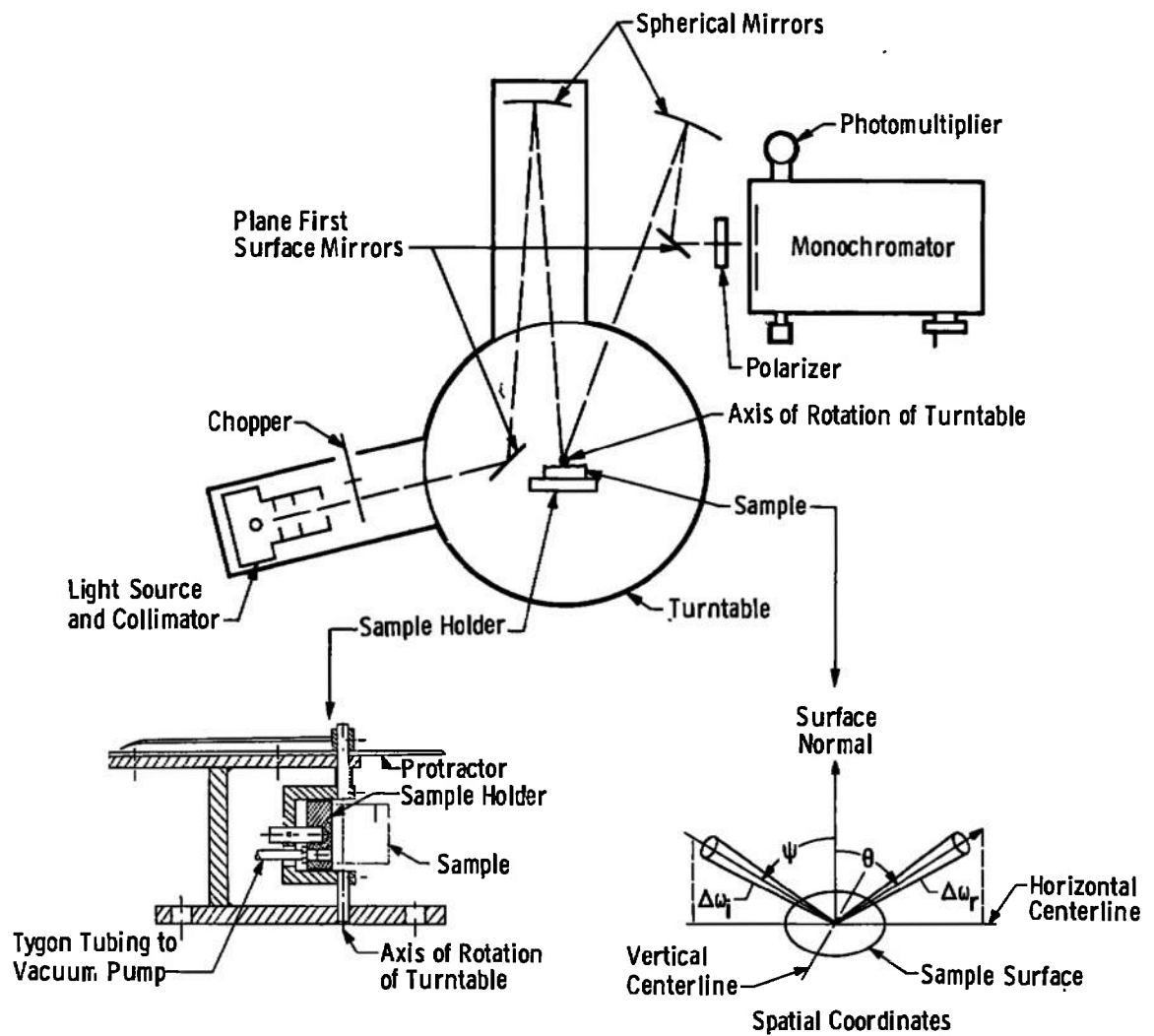
APPENDIX
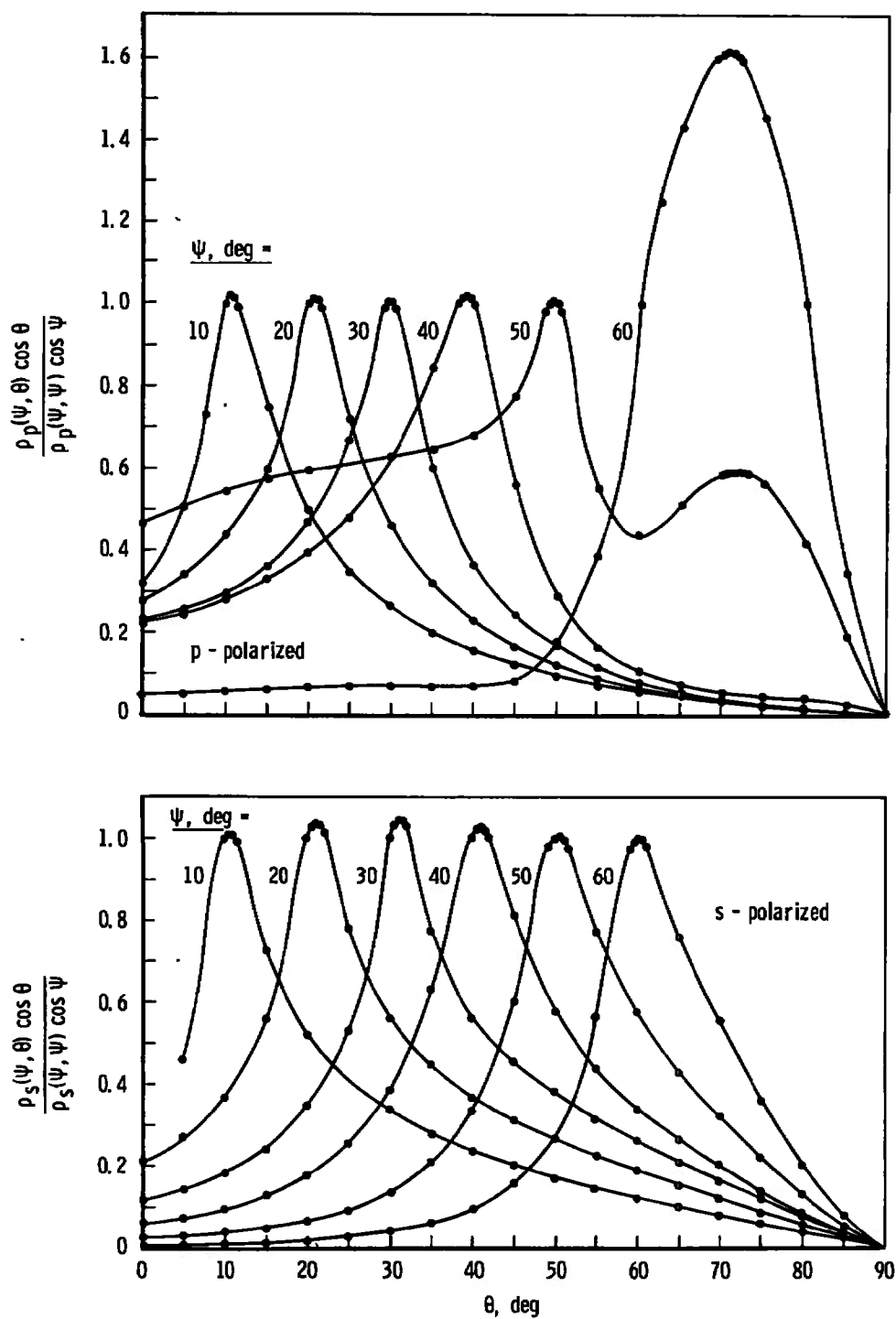**ILLUSTRATIONS**

Fig. 1 Schematic of Experimental Apparatus

Fig. 2 Directional Distributions of Plane-Polarized Radiant Flux Reflected from Roughened Glass Surface, σ_m = 0.34μ, λ = 5μ, Various Incidence Angles ψ
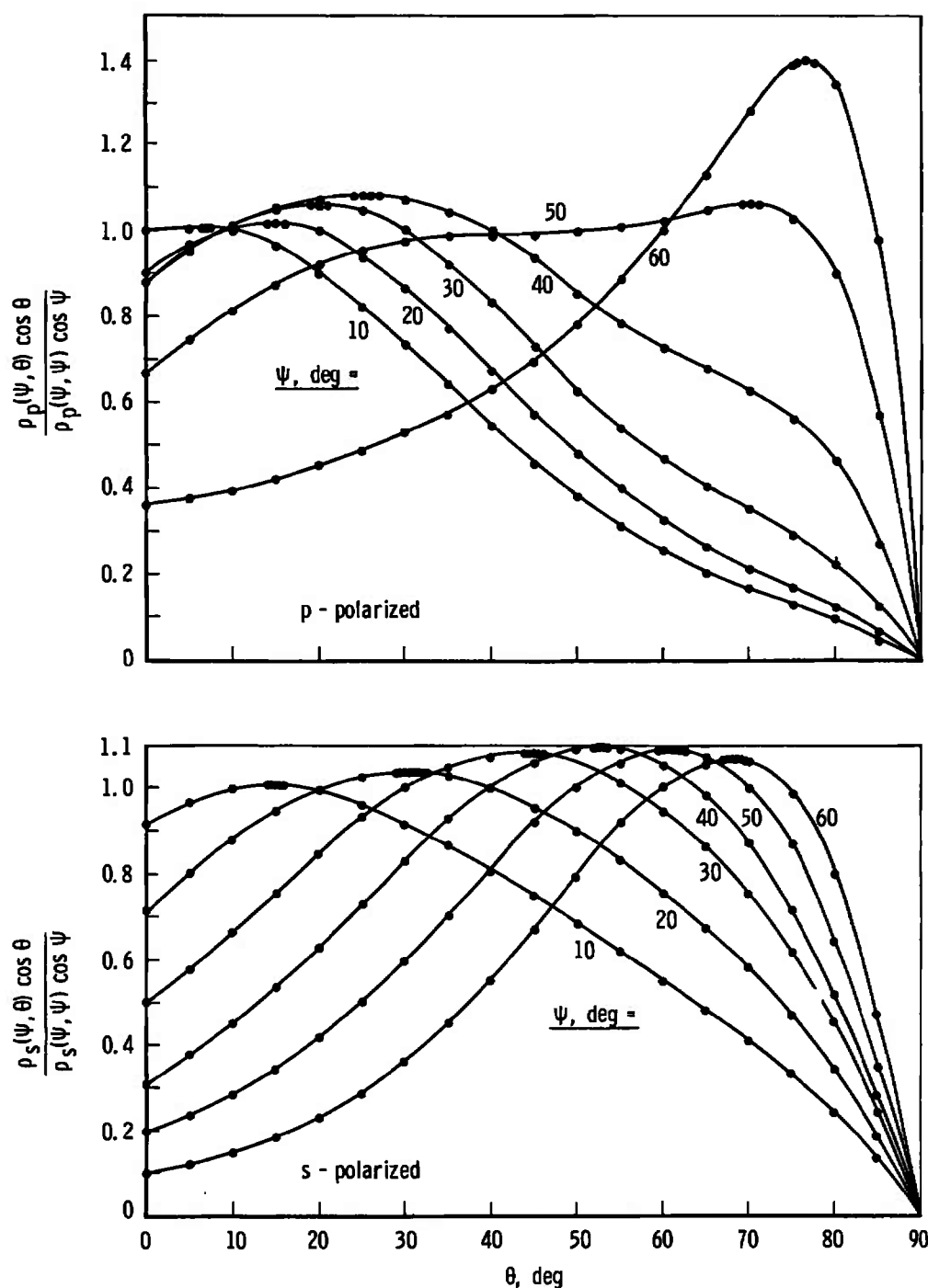
Fig. 3 Directional Distributions of Plane-Polarized Radiant Flux Reflected
from Roughened Glass Surface, σ_m = 1.77μ, λ = 0.5μ,
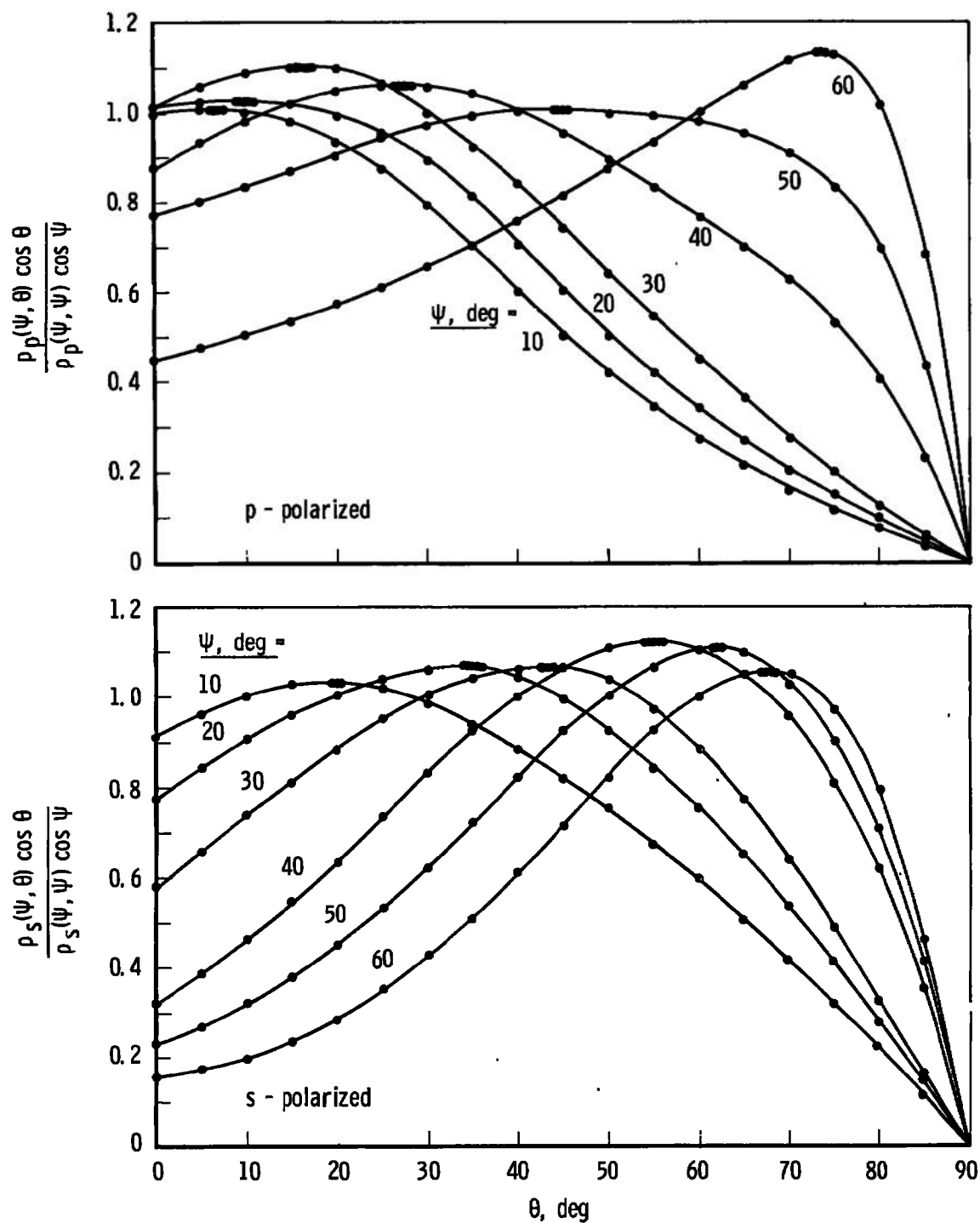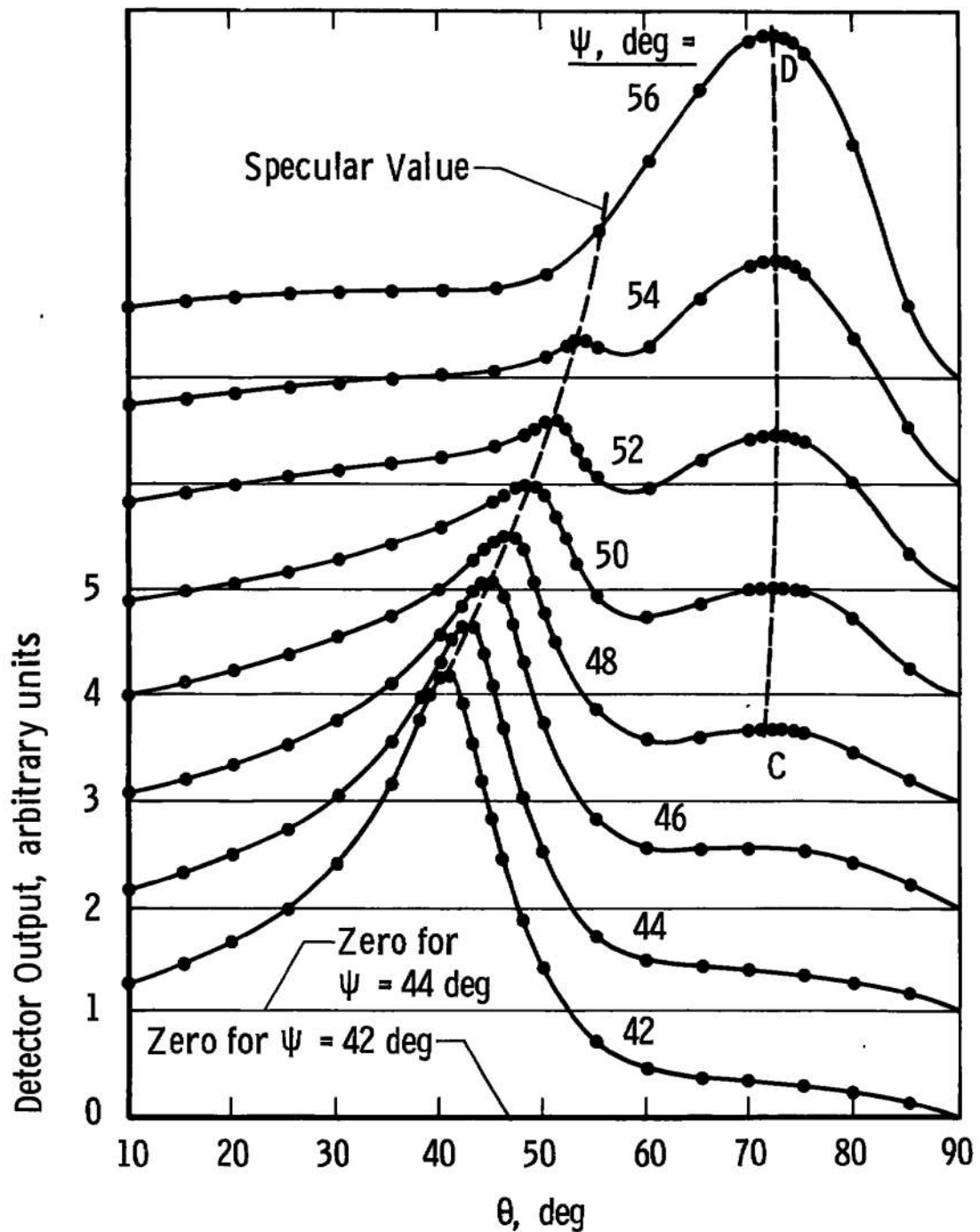Various Incidence Angles ψ

Fig. 4 Directional Distributions of Plane-Polarized Radiant Flux Reflected from Roughened Glass Surface, $\sigma_m = 3.35\mu$, $\lambda = 0.5\mu$, Various Incidence Angles ψ

Fig. 5 Directional Distributions of p-Polarized Radiant Flux Reflected
from Roughened Glass Surface, $\sigma_m = 0.34\mu$, $\lambda = 0.5\mu$,
Incidence Angles near the Brewster Angle
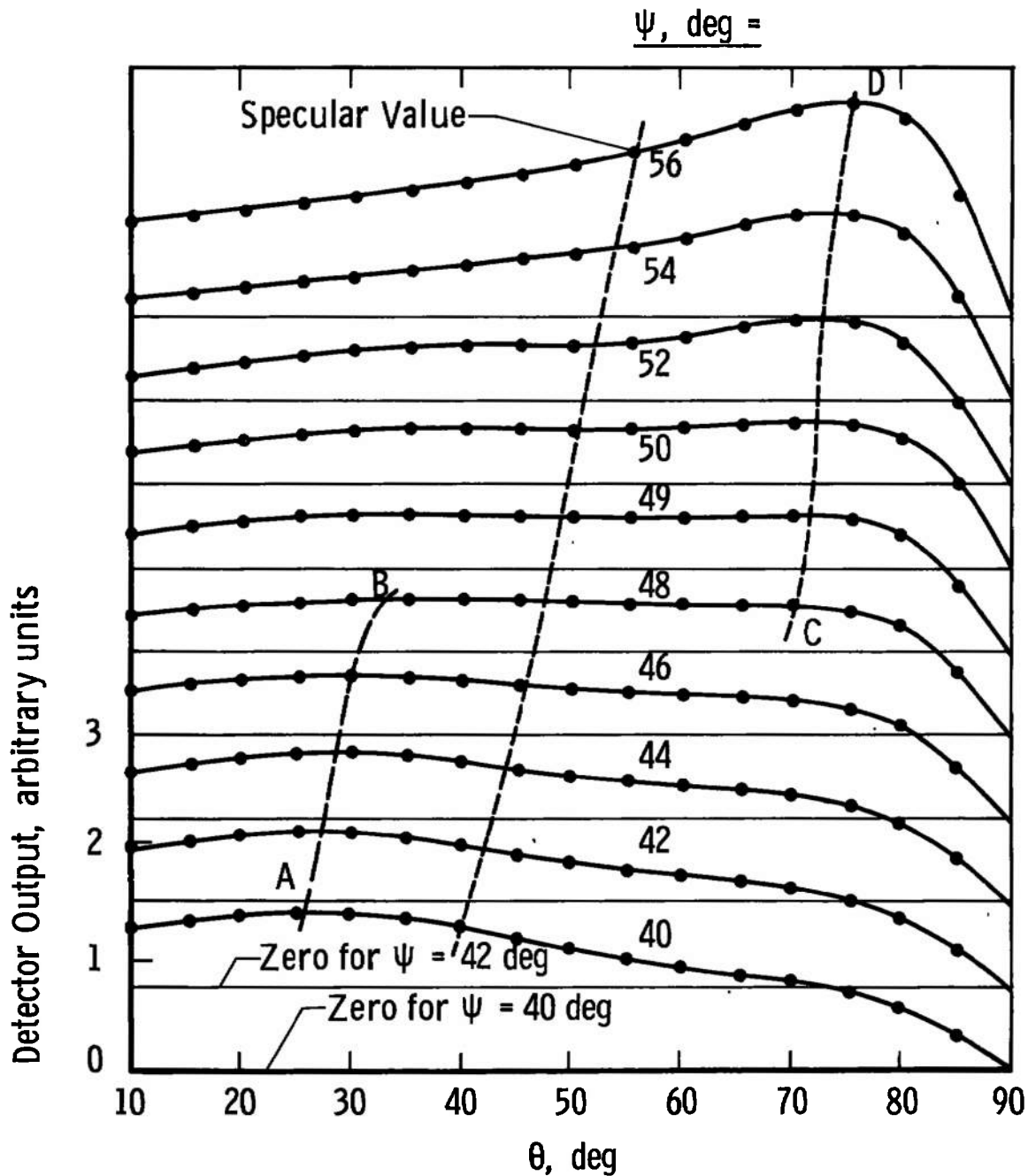
Note: Sliding origin is used.

Fig. 6 Directional Distributions of p-Polarized Radiant Flux Reflected from Roughened Glass Surface, $\sigma_m = 1.77\mu$, $\lambda = 0.5\mu$, Incidence Angles near the Brewster Angle
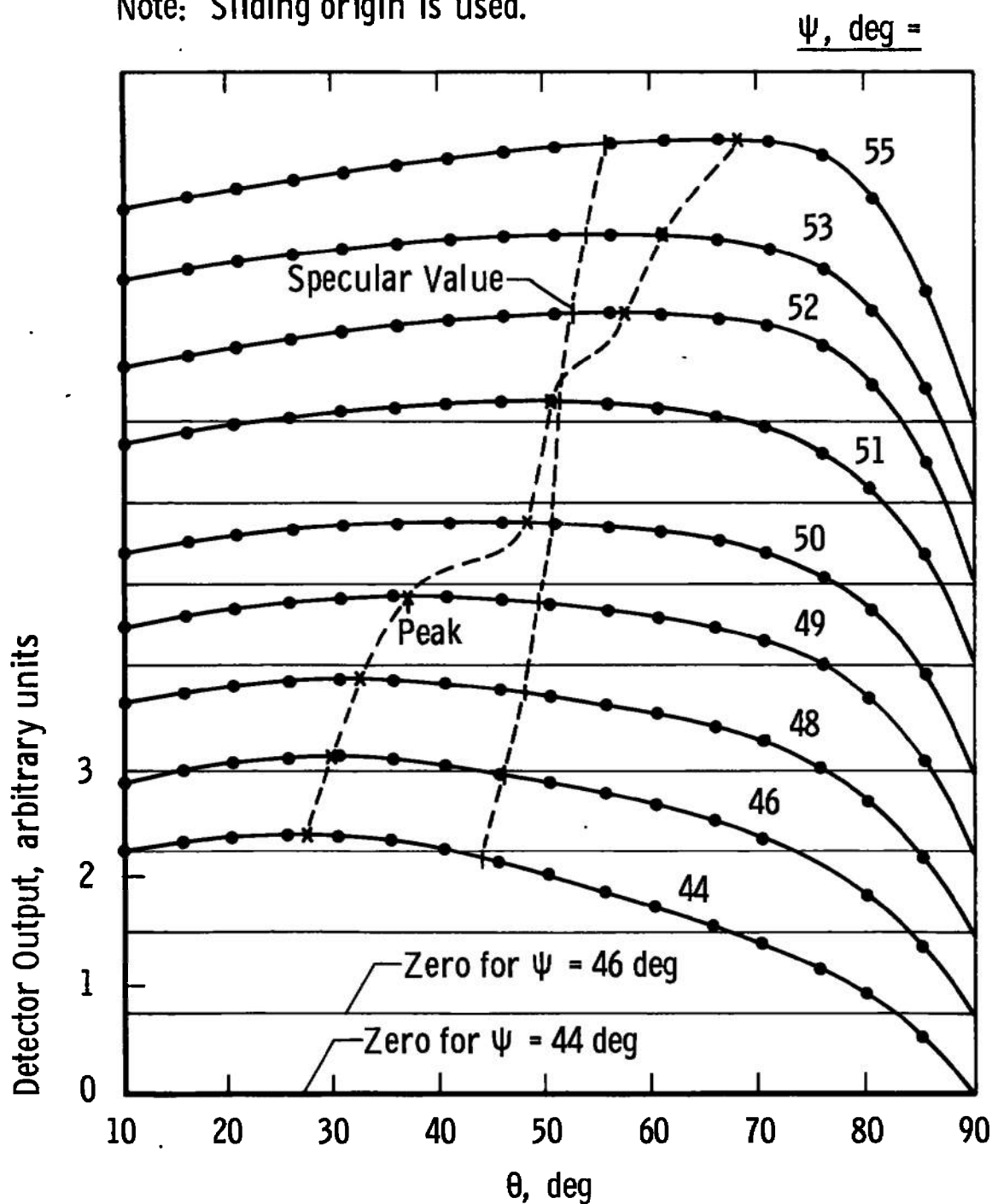
Note: Sliding origin is used.

ψ, deg =

Fig. 7 Directional Distributions of p-Polarized Radiant Flux Reflected from Roughened Glass Surface, $\sigma_m = 3.35\mu$, $\lambda = 0.5\mu$, Incidence Angles near the Brewster Angle
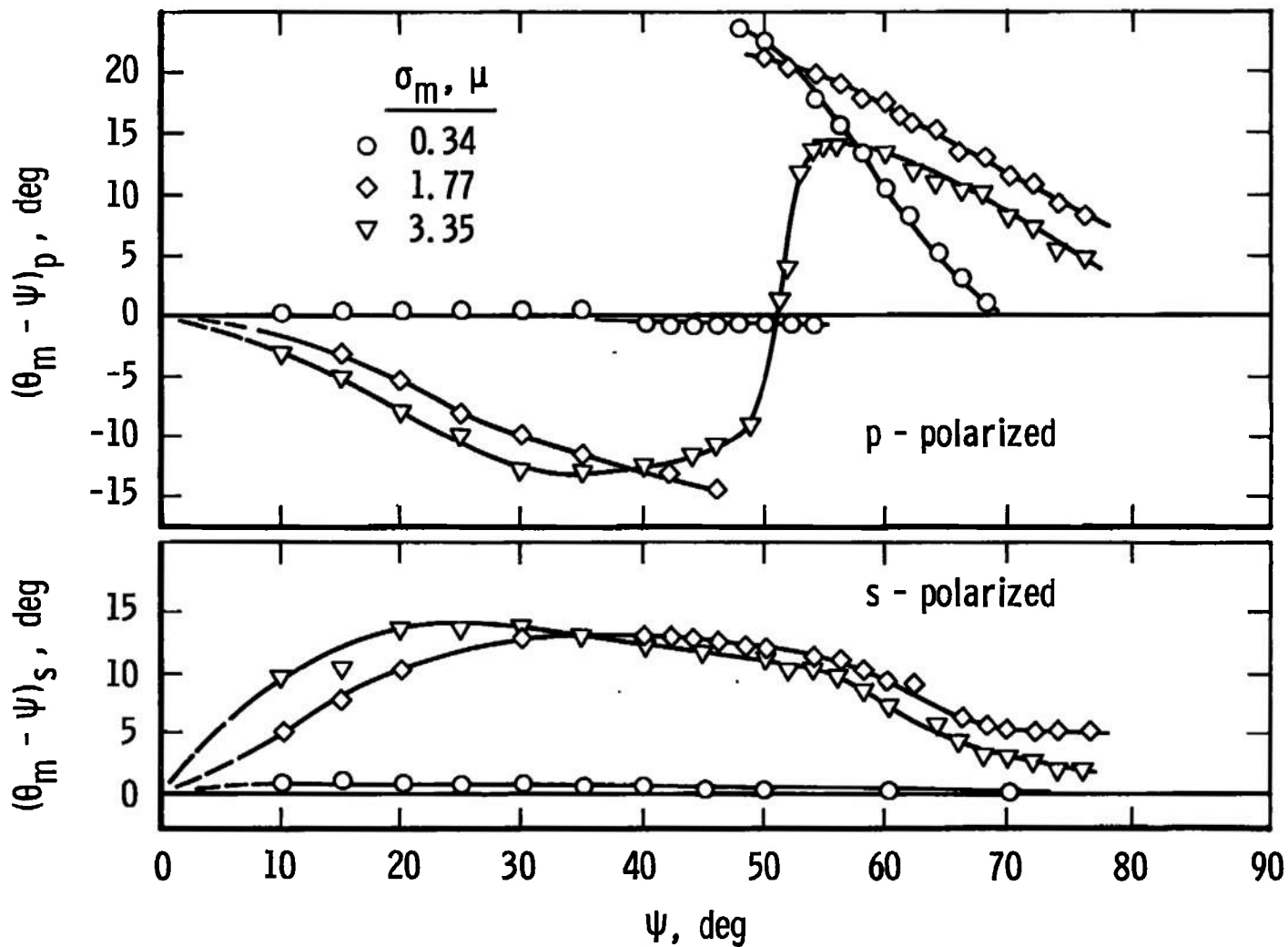
Fig. 8 Measured Angular Displacements (Relative to the Specular Direction)
of Off-Specular Maxima in the Distributions of Plane-Polarized Radiant
Flux Reflected from Roughened Glass Surfaces, $\lambda = 0.5\mu$. Various
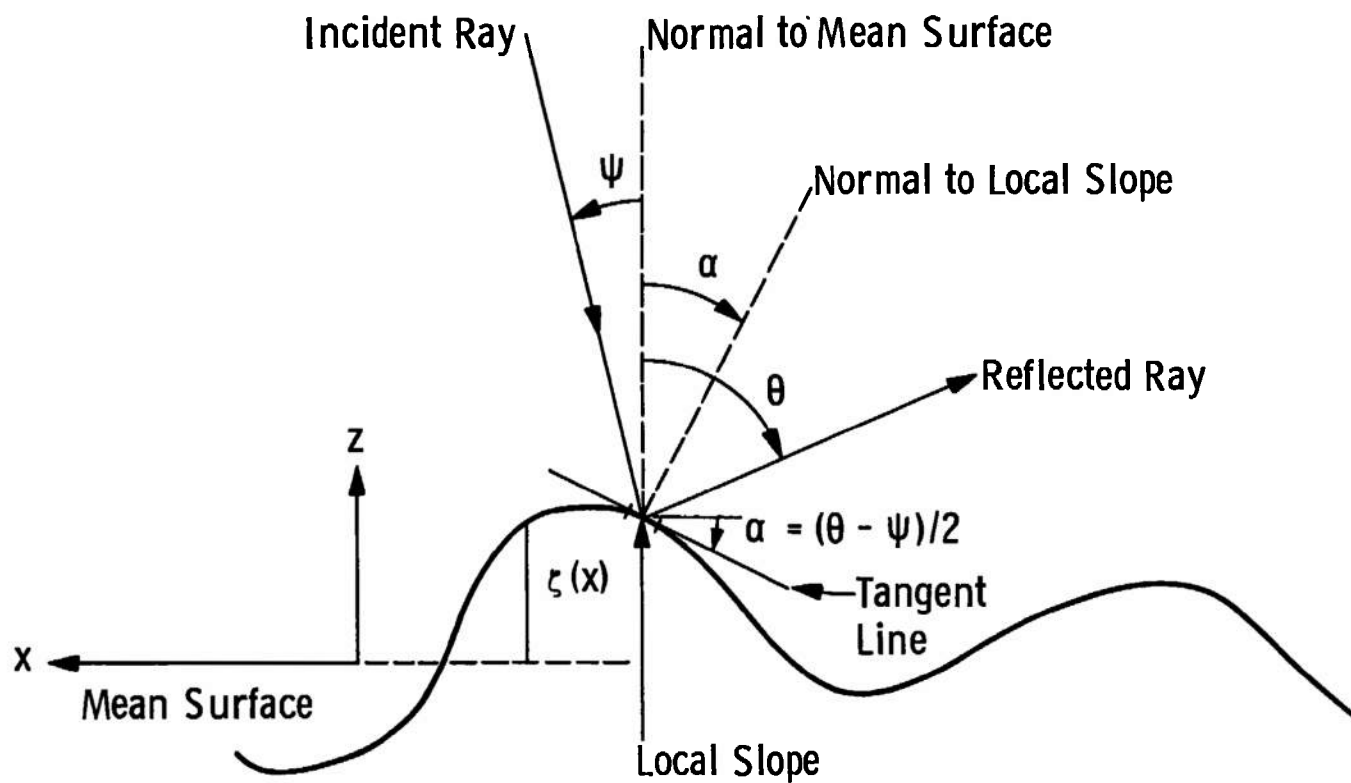Surface Roughnesses σ_m and Incidence Angles ψ

Fig. 9 Sketch of Ray Reflection from Single Local Slope of Rough Surface

Fig. 10 Comparison between Theoretical and Experimental Distributions of Polarized Radiant Flux Reflected from Roughened Glass Surface for Incidence Angle of 20 deg
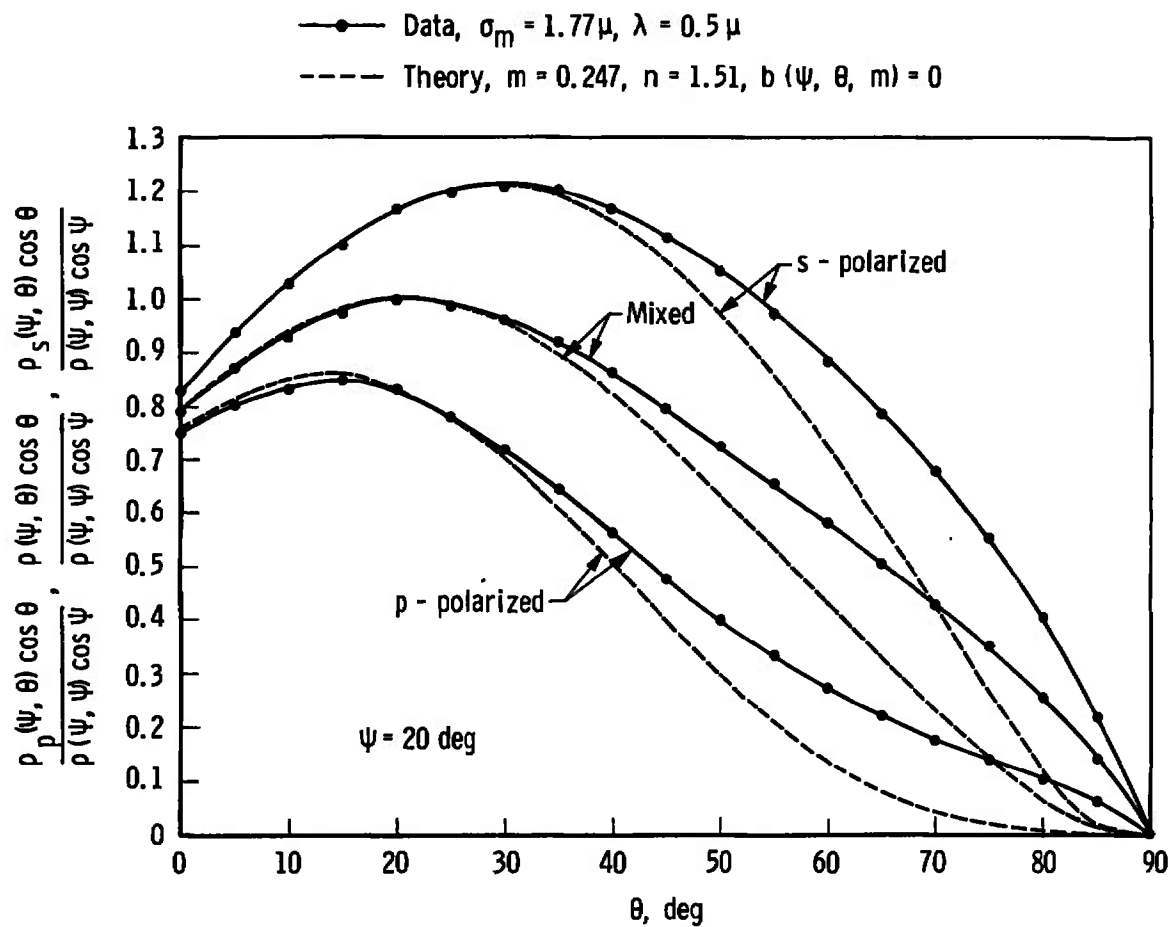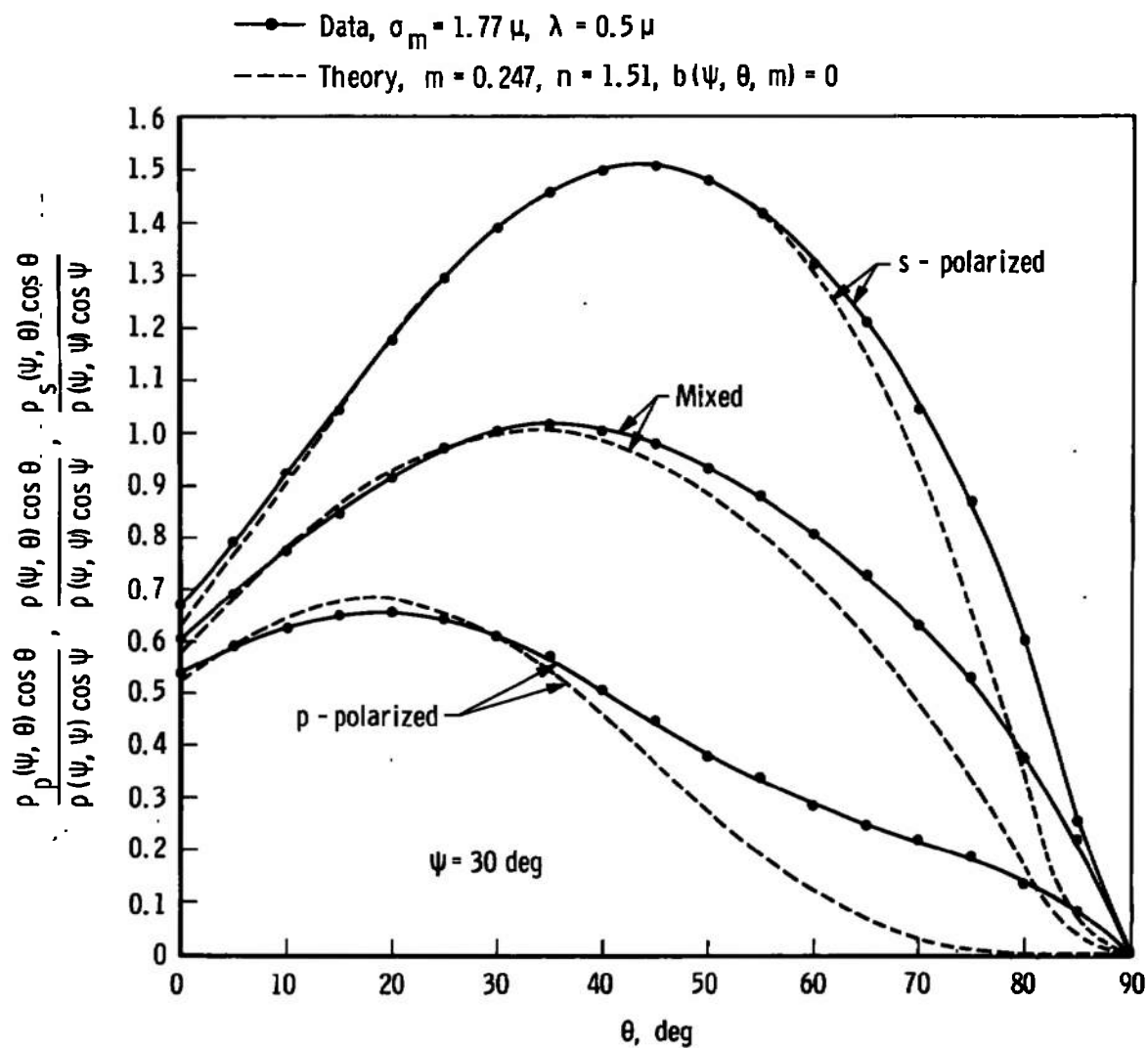
Fig. 11 Comparison between Theoretical and Experimental Distributions of
Polarized Radiant Flux Reflected from Roughened Glass Surface for
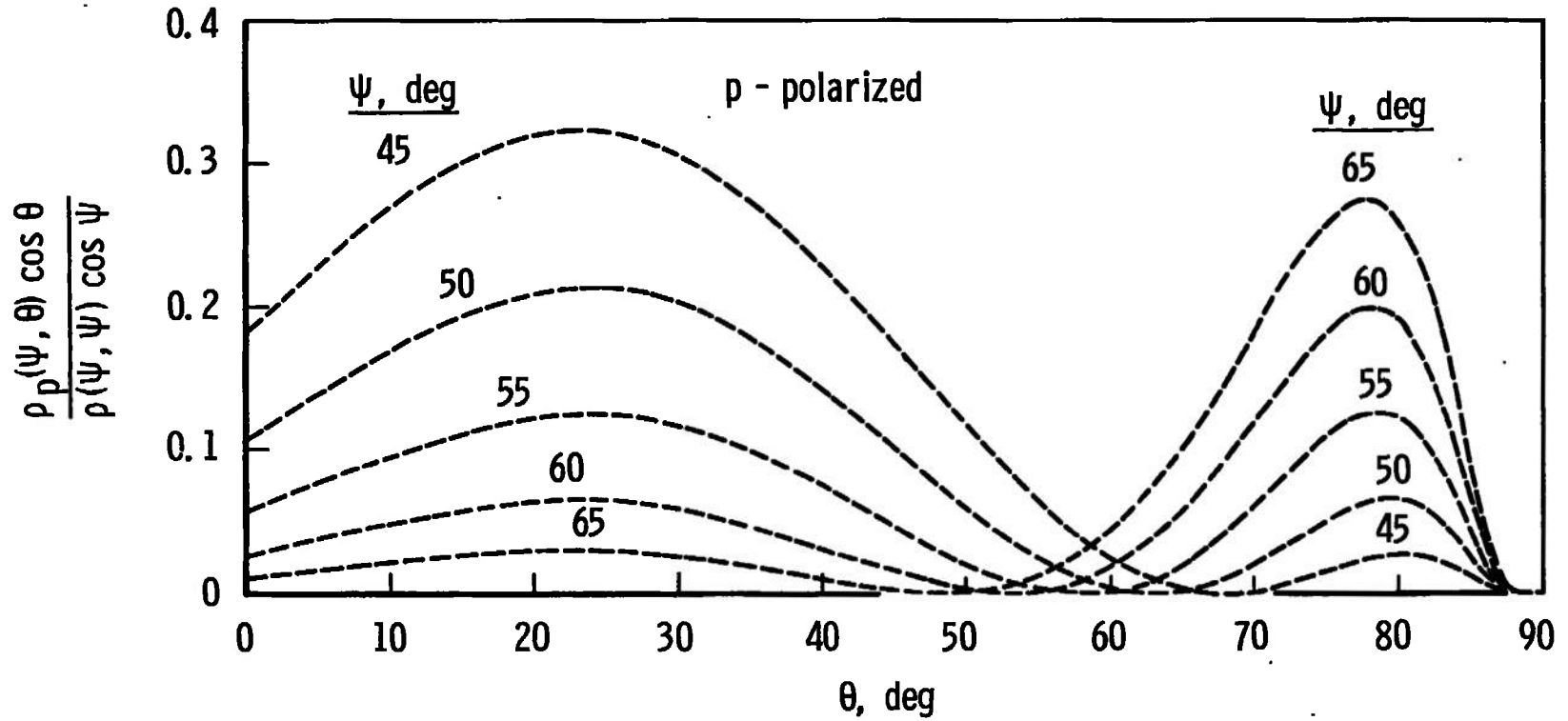Incidence Angle of 30 deg

Fig. 12 Theoretical Distributions of p-Polarized Radiant Flux Reflected from
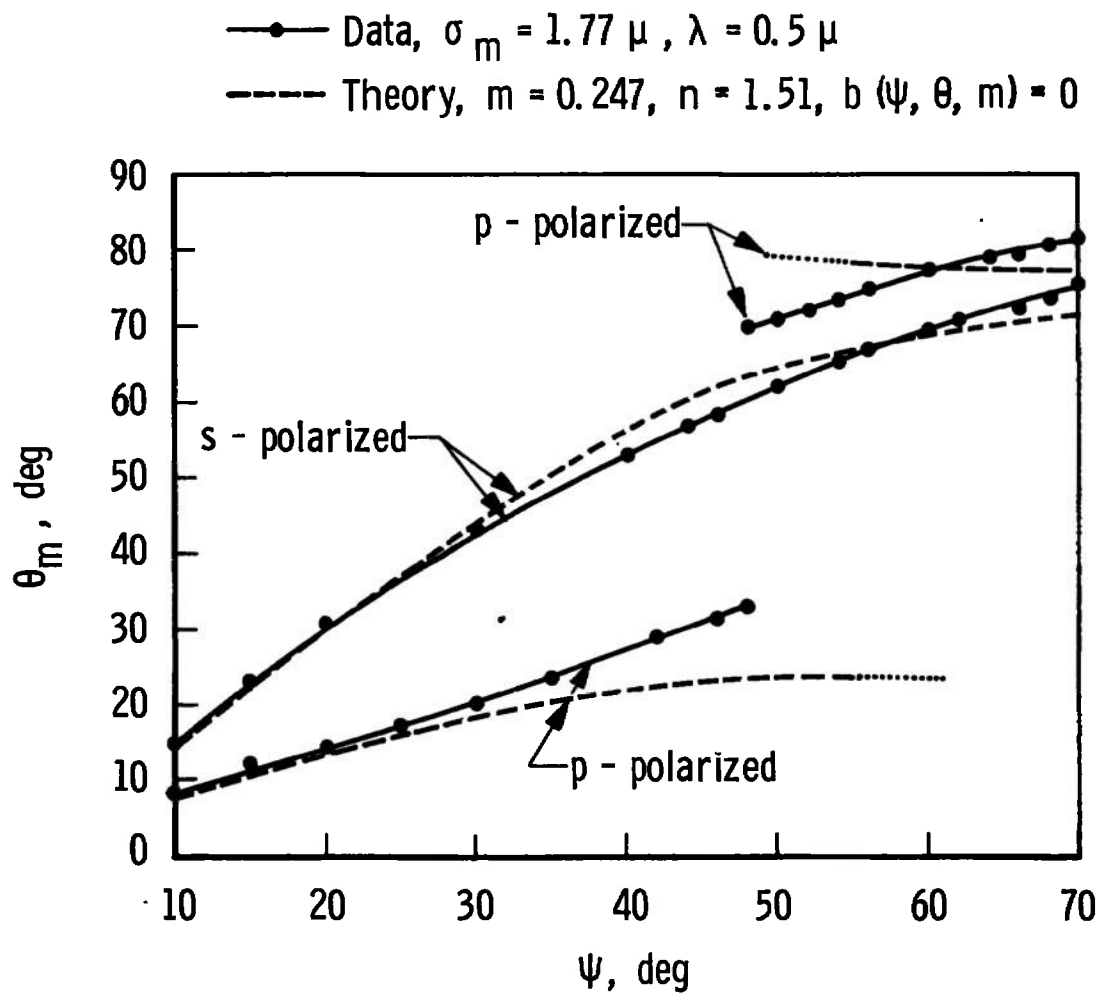Roughened Dielectric Surface for Incidence Angles near the Brewster Angle

Fig. 13 Comparison between Angular Locations of the Off-Specular Maxima of Theoretical and Experimental Distributions of Plane-Polarized Radiant Flux Reflected from Roughened Glass Surface. Various Incidence Angles ψ

DOCUMENT CONTROL DATA - R & D		

(Security classification of title, body of abstract and indexing annotation must be entered when the overall report is classified)

1. ORIGINATING ACTIVITY *(Corporate author)*	2a. REPORT SECURITY CLASSIFICATION
Arnold Engineering Development Center, ARO, Inc., Operating Contractor, Arnold Air Force Station, Tennessee 37389	UNCLASSIFIED
	2b. GROUP
	N/A

3. REPORT TITLE

SUPER- AND SUB-SPECULAR MAXIMA IN THE ANGULAR DISTRIBUTION OF POLARIZED RADIATION REFLECTED FROM ROUGHENED DIELECTRIC SURFACES

4. DESCRIPTIVE NOTES *(Type of report and inclusive dates)*

May 1969 through April 1970 - Final Report

5. AUTHOR(S) *(First name, middle initial, last name)*

A. M. Smith and P. R. Muller, ARO, Inc.

6. REPORT DATE	7a. TOTAL NO. OF PAGES	7b. NO. OF REFS
March 1971	31	15

8a. CONTRACT OR GRANT NO. F40600-71-C-0002	9a. ORIGINATOR'S REPORT NUMBER(S)
b. Program Element 64719F	AEDC-TR-70-286
	9b. OTHER REPORT NO(S) *(Any other numbers that may be assigned this report)*
	ARO-VKF-TR-70-286

10. DISTRIBUTION STATEMENT

This document has been approved for public release and sale; its distribution is unlimited.

11. SUPPLEMENTARY NOTES	12. SPONSORING MILITARY ACTIVITY
Available in DDC.	Arnold Engineering Development Center (XON), Air Force Systems Command, Arnold Air Force Station, Tenn. 37389

13. ABSTRACT   To study the effects of surface roughness on the reflection of radiation from the vacuum-deposit interface of CO_2 cryodeposits, detailed angular distribution measurements were made of the polarized radiant flux reflected from roughened glass samples which had similar optical properties to CO_2 cryodeposits. As a result of these measurements, a new type of off-specular peak was discovered. This maximum is termed "sub-specular" and occurs for parallel-polarized radiation provided the wavelength and zenith incidence angle are appreciably less than the dielectric's surface roughness and Brewster angle, respectively. If the incidence angle is greater than the Brewster angle, the maximum in the angular distribution is super-specular and occurs even for a surface roughness smaller than the radiation wavelength. No sub-specular maxima are observed for perpendicular-polarized radiation, but super-specular maxima occur for all non-normal incidence angles provided the dielectric's surface roughness is significantly greater than the radiation wavelength, 0.5μ. For reflected radiant flux containing all components of polarization, only super-specular peaks are observed. These peaks occur if the dielectric surface roughness is larger than the radiation wavelength and the incidence angle is equal to or greater than approximately 30 deg. A formula is derived for the radiation reflected in the plane of incidence and is used to quantitatively confirm the existence of the super- and sub-specular maxima for moderate incidence angles. The super- and sub-specular maxima phenomena have potential application to making in situ measurements of surface roughness characteristics.

14. KEY WORDS	LINK A		LINK B		LINK C	
	ROLE	WT	ROLE	WT	ROLE	WT
off-specular reflection						
surface roughness						
polarized radiation						
angular distribution						

AF4
Arnold AFS Tenn